

# Optical Modulator using Ultra-Thin Silicon Waveguide in SOI Hybrid Technology

Ahmed B. Ayoub

The American University in Cairo

Mohamed Swillam (✉ [m.swillam@aucegypt.edu](mailto:m.swillam@aucegypt.edu))

The American University in Cairo <https://orcid.org/0000-0002-7962-2341>

---

## Short Report

**Keywords:** interference, modulation, photonic structures, Mach-Zehnder Interferometer, ultra-thin.

**Posted Date:** August 12th, 2021

**DOI:** <https://doi.org/10.21203/rs.3.rs-597330/v1>

**License:**   This work is licensed under a Creative Commons Attribution 4.0 International License.

[Read Full License](#)

---

**Version of Record:** A version of this preprint was published at Optical and Quantum Electronics on February 25th, 2022. See the published version at <https://doi.org/10.1007/s11082-021-03467-w>.

1       **Optical Modulator using Ultra-Thin Silicon Waveguide in**  
2                                   **SOI Hybrid technology**

3  
4   Ahmed B. Ayoub <sup>a</sup>, and Mohamed A. Swillam <sup>a,\*</sup>

5   <sup>a</sup>Department of Physics, School of Sciences and Engineering, American University in  
6   Cairo, Cairo 11830, Egypt.

7  
8  
9   **Acknowledgements**

10   This work was made possible by a NPRP award [NPRP 7-456-1-085] from the Qatar National Research Fund  
11   (member of the Qatar Foundation). The statements made herein are solely the responsibility of the authors.

12   **Conflict of interest**

13   The authors declare that they have no conflict of interest.

14   **Author Contributions**

15   A..b. Ayoub conceived the basic idea and validated the concept of operation through computer-aided simulations.  
16   M.A. Swillam supervised the entire project. All the authors contributed to the general discussion and revision of  
17   the manuscript.

18  
19   **Availability of data and material.** Authors will make readily reproducible materials described in  
20   the manuscript, including new software, databases and all relevant raw data, freely available to any  
21   scientist wishing to use them, without breaching participant confidentiality. Authors will make  
22   their new software, databases, application/tool described in the manuscript available for testing by  
23   reviewers in a way that preserves the reviewers' anonymity.

44  
45  
46  
47  
48  
49  
50

51 **Abstract.** We propose a detailed study of an on-chip optical modulator using a non-  
52 conventional silicon-based platform. This platform is based on the optimum design of  
53 ultra-thin silicon on insulator (SOI) waveguide. This platform is characterized by low  
54 field confinement inside the core waveguide and high sensitivity to the cladding  
55 index. Accordingly, it lends itself to a wide range of applications, such as sensing and  
56 optical modulation. By employing this waveguide into the Mach-Zehnder  
57 interferometer (MZI) configuration, an efficient optical modulator is reported using an  
58 organic polymer as an active material for the electro-optic effect. An extinction ratio  
59 of more than 20 dB is achieved with energy per bit of 13.21 fJ/bit for 0.5 V applied  
60 voltage. This studied platform shows promising and adequate performance for  
61 modulation applications. It is cheap and easy to fabricate.

62

63 **Keywords:** interference, modulation, photonic structures, Mach-Zehnder  
64 Interferometer, ultra-thin.

65

66 **\*Address all correspondence to** Mohamed A. Swillam, The American University in  
67 Cairo, Department of Physics, AUC Avenue New Cairo, Cairo, Egypt, P.O. Box 74;  
68 Tel:+202-2615-2612; E-mail: m.swillam@aucegypt.edu.

69

## 70 1 INTRODUCTION

71 Silicon Photonics is a CMOS-compatible platform technology that is power-efficient  
72 while approaching operating speed comparable to that of light [1]. Aiming at high-  
73 bandwidth systems with high operating speed, electronic and photonic circuits were  
74 integrated as in data-communication systems, which resulted in systems with  
75 outstanding speed rates and lower power losses. Besides, photonic integrated circuits  
76 have been employed in different applications, including optical modulation, and  
77 sensing [1-3].

78 Optical modulators play a vital role in optoelectronic systems. Thanks to these  
79 components, electronic signals are converted to optical signals that propagate using  
80 optical waveguides [1]. Commonly, optical modulation is done either through an  
81 Electro-optic effect (i.e., Pockels, Kerr) or a thermo-optic effect [1]. While silicon  
82 lacks electro-optic effects, it has a high thermo-optical property at low speed (i.e., it  
83 cannot be employed in high-speed communication systems) [4].

84 Recently, various photonic based modulating structures have been demonstrated [5,  
85 6]. A silicon-organic hybrid modulator was proposed [5] that operates at frequencies  
86 up to 100 GHz and beyond so that it can be used in electronic-photonic processing at  
87 high speed. Despite its large length of 500  $\mu\text{m}$ , phase efficiency of 11 V.mm, and a  
88 capacitance per length of about 100 fF/mm with a parasitic resistance of few Giga-  
89 ohms. A high-speed silicon Mach-Zehnder modulator (MZM) with a low insertion  
90 loss of 1.9 dB was demonstrated [6]. Phase efficiency of less than 2 V.cm was  
91 achieved despite an arm length of 750  $\mu\text{m}$ . High-performance modulation with an  
92 extinction ratio of 7.5 dB was delivered at 50 Gbps at the expense of an additional  
93 optical loss.

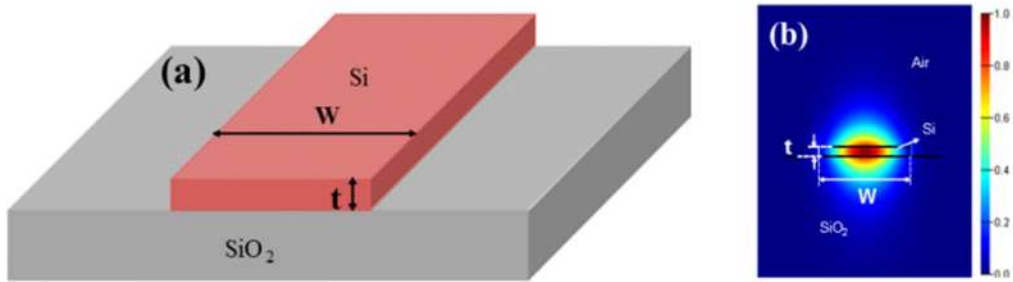
94 From the previous examples, it is observed that achieving a high-performance  
95 photonic structure is considered a tradeoff between the size, loss, and fabrication  
96 complexity of photonics modulators. Most of the current silicon photonics-based  
97 modulators are based on few hundreds of nanometer waveguide width that requires  
98 electron beam lithography technology (EBL) for fabricating these waveguides.  
99 Alternatively, it can be fabricated with a high-quality mask with a submicron  
100 dimension. However, this mask is also expensive and requires specialized technology  
101 to be produced.

102 Therefore, the need for a new platform for designing photonic structures with standard  
103 fabrication technology is necessary. With the proposed platform, standard and  
104 straightforward fabrication technology can be employed to fabricate structures with  
105 dimensions of more than 1.0 microns. Allowing for standard technology for mask  
106 preparation and effectively alleviate the need for EBL technology. On the other hand,  
107 the suggested platform also has a unique feature for being more sensitive than other  
108 larger waveguide platforms such as ridge configuration, as will be explained through  
109 the manuscript.

110 The paper is organized as follows: section (2) describes the properties of the proposed  
 111 platform, section (3) studies the photonic modulator based on the proposed platform,  
 112 and finally, section (4) concludes the paper.

## 113 2 ULTRA THIN WAVEGUIDE PROPERTIES

114 Several studies previously proposed a similar platform to the one proposed in this  
 115 work [7-13]. The proposed platform is based on an ultra-thin SOI that supports the  
 116 fundamental mode, as would be seen in a conventional SOI ( $t=220$  nm,  $W=400$ nm).  
 117 The silicon waveguide is shown in Fig. 1, it has a thin thickness ( $t$ ) of only 50 nm.



118  
 119 **Fig. 1** SOI ultra-thin waveguide structure. (a) Schematic for the physical dimensions  
 120 of the ultra-thin waveguide. (b) Mode profile for the ultra-thin SOI.

121 The ultra-thin SOI technology supports only the TE mode owing to the small  
 122 thickness. TE mode is defined by the mode whose major component is along the  
 123 longer dimension in the plane of incidence (major electric field component along  
 124 “W”). Due to the small thickness, the TE mode has a low confinement factor inside  
 125 the waveguide as shown in Fig. 1(b) [10-13]. The mode profile in Fig. 1(b) was  
 126 calculated using the mode solver of Lumerical [14]. On the other hand, TM mode  
 127 (i.e., major electric field component along “t”) can be supported by expanding the  
 128 thickness ( $t$ ) of the waveguide as in a conventional waveguide that has a thickness of  
 129 220nm. However, if  $t=50$ nm, regardless of ( $W$ ), TM mode will not be supported by  
 130 the waveguide.

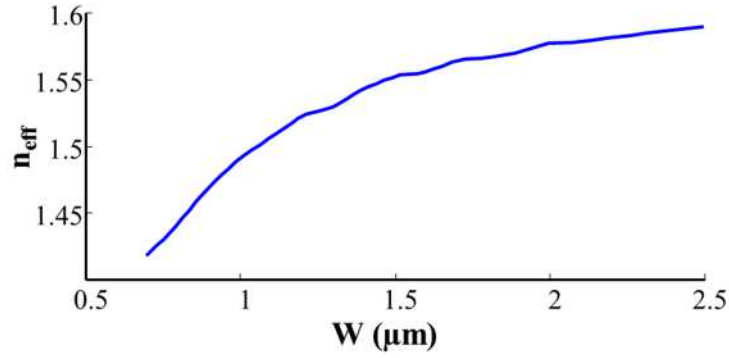
131 In the SOI geometry, it is assumed that the surrounding is air, while the substrate is  
 132 silicon dioxide ( $\text{SiO}_2$ ) with a thickness of  $1 \mu\text{m}$  to avoid leakage to the silicon wafer.  
 133 Substrate leakage loss attenuation is given by the following equation (1) [15]:

$$134 \quad \alpha_{leak} = e^{-2\left(\sqrt{n_{eff}^2 - n_0^2}\right)k_0 A} \quad (1)$$

135 where  $k_0 = \frac{2\pi}{\lambda_0}$  is the free space wavenumber,  $n_{eff}$  is the effective index of the mode,  
136  $n_0$  is the effective index of the oxide layer, and  $A$  is the thickness of the oxide, in  
137 which for the given parameters ( $\lambda_0=1550\text{nm}$ ,  $n_{eff}=1.55$ ,  $n_0=1.45$ ,  $A=1 \mu\text{m}$ ),  $\alpha_{leak} =$   
138 **0.011**. Such value can be further suppressed by increasing the thickness ( $A$ ) to 2 – 3  
139  $\mu\text{m}$ .

140 Modal analysis was done by varying the dimensions of the waveguide cross-section  
141 using mode solver of Lumerical [14]. The effect of changing the width of the  
142 waveguide “W” on the effective refractive index of the structure while keeping  $t=50$   
143 nm is shown in Fig. 2. Only the first fundamental mode is supported with  $700\text{nm} < W$   
144  $< 2\mu\text{m}$ , no modes are supported when  $W < 700$  nm. On the other hand, multi-modes  
145 are supported given  $W > 2 \mu\text{m}$ . Throughout the paper, silicon waveguide with  
146 parameters ( $t=50$  nm,  $W=2 \mu\text{m}$ ) will be used. This waveguide can be fabricated using  
147 the standard fabrication process for the conventional waveguide. The fabrication steps  
148 are performed as follows: (1) performing a partial etching on silicon on insulator  
149 platform to get the required thickness (i.e.,  $t=50$  nm), (2) then performing mask  
150 lithography, (3) development of the wafer, (4) performing the dry etching process to  
151 etch the unneeded Si layer, and (5) finally remove the etchant to reach the final  
152 structure. Fabrication tolerance will not affect the overall performance, as seen in Fig.  
153 2 in which the  $n_{eff}$  is not oscillating as a function of the width, the fact that  
154 compensates the fabrication tolerances due to large width.

155 During the computational analysis, the MZI has an arm length of  $350 \mu\text{m}$  and a  
156 bending radius of  $80 \mu\text{m}$ . The propagation loss is calculated for the waveguide to  
157 know the limitations on the arm length. A propagation loss of 0.024 dB/cm is  
158 considered an acceptable value for the design of long-arm modulators. However,  
159 additional terms can include the bending loss of the MZI, which is in the range of 2.5  
160 dB/cm at a bending radius of  $80 \mu\text{m}$ . Adding a surface roughness of 3 dB/cm can  
161 result in a total loss of around 0.2 dB for an arm length of  $350 \mu\text{m}$ . In the following  
162 section, an ultra-thin MZI optical modulator is discussed in detail. A comparison with  
163 other modulation systems is also performed.



164

165 **Fig. 2** The effect of changing the waveguide width on the effective index. The  
 166 substrate is assumed to be SiO<sub>2</sub> with air as the surrounding.

### 167 3 ULTRA THIN WAVEGUIDE BASED PHOTONIC MODULATOR

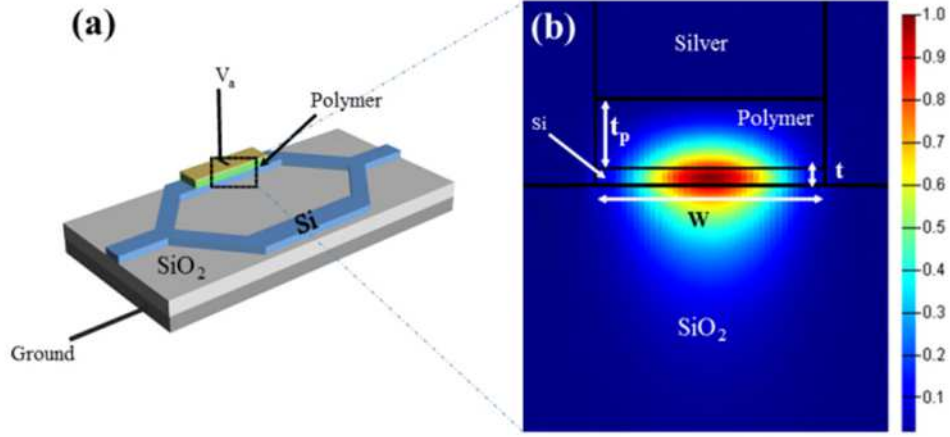
#### 168 3.1 MZI based Photonic Modulator

169 Electromagnetic simulations are performed using the commercial Beam Propagation  
 170 Method (BPM) [16]. Assuming polymer with the Pockels electro-optic effect,  
 171 refractive index change is governed by equation (2) [17]:

$$172 \quad \Delta n = \frac{1}{2} n_0^3 r_{33} \frac{V_a}{t_p} \quad (2)$$

173 where  $n_0$  is the polymer refractive index at zero applied voltage and has a value of 1.6,  
 174  $V_a$  is the applied voltage,  $t_p$  is the thickness of the polymer,  $r_{33}$  represent the electro-  
 175 optic effect and has a value of 310 pm/V. This polymer can be retrieved by a 1:1  
 176 mixture between (C<sub>28</sub>H<sub>21</sub>F<sub>3</sub>N<sub>4</sub>O<sub>5</sub>, molecular weight 518.6) and (C<sub>32</sub>H<sub>28</sub>F<sub>3</sub>N<sub>4</sub>O,  
 177 molecular weight 541.6), as discussed in Ref. 18. Having  $t_p = 200 \text{ nm}$ , resulted in a  
 178 calculated metal absorption loss of 24dB/cm, yielding a total metal absorption loss of  
 179 0.84 dB for an arm length of 350  $\mu\text{m}$ . “On” state is reached when applying voltage  $V_a$   
 180 = 2V through the metal electrodes resulting in a refractive index change of  $\Delta n =$   
 181  $6.35 * 10^{-3}$ , as given by equation (2).

182 The schematic of the optical modulator design is shown in Fig. 3(a). As discussed in  
 183 the previous section, the TE mode is weakly confined in the ultra-thin waveguide,  
 184 allowing for better penetration into the polymer, as shown in Fig. 3(b). Field  
 185 distribution is calculated using the mode solver of Lumerical [14]. High field  
 186 penetration into the polymer allows for a higher extinction ratio at significantly  
 187 shorter arm length as compared to conventional SOI systems.



188

189 **Fig. 3** MZI photonic modulator. (a) Schematic for the ultra-thin SOI modulator. (b)  
 190 mode profile inside the polymer, it shows the strong interaction between the optical  
 191 mode and the polymer.

### 192 3.2 Modulator Results

193 As mentioned in the previous section, during the computational analysis, the arm  
 194 length was designed to be 350  $\mu\text{m}$  with a bending radius of 80  $\mu\text{m}$ , with a polymer  
 195 thickness " $t_p$ " of 200 nm yielding an acceptable capacitance (C) value of 79.27 Ff  
 196 without dramatically suppressing the performance [12]. Assuming bit-rate ( $R_{bit}$ ) of  
 197 0.1Tbit/sec, the power consumption for a return to zero (RTZ) can be calculated using  
 198 equation (3) [19]:

$$199 \quad P = \frac{1}{2} R_{bit} C V_a^2 \quad (3)$$

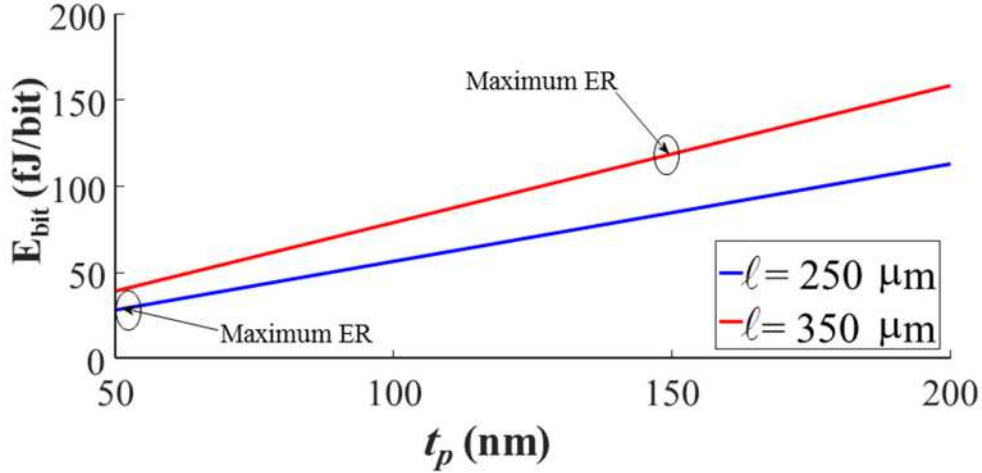
200

201 Assuming applied voltage  $V_a=2\text{V}$ ,  $P = 0.0158\text{W}$ . Hence, ( $E_{bit} = \frac{1}{2} C V_a^2$ ) equals 158  
 202 fJ/bit [12]. The half-wave voltage  $V_\pi$  is calculated using equation (4):

$$203 \quad V_\pi = \frac{\lambda_0 t_p}{n_0^3 r_{33} \zeta} \quad (4)$$

204 ,where  $\zeta$  is the arm length, Given the above parameters,  $V_\pi = 0.697\text{ V}$  and  $V_\pi \zeta =$   
 205  $2.44 * 10 - 2\text{ V.cm}$ . At an  $\lambda_0 = 1550\text{ nm}$ , the extinction ratio (ER) equals 11.3 dB  
 206 which is given by  $ER = 10 \log \frac{P_{on}}{P_{off}}$ ; where  $P_{on}, P_{off}$  is the power in the "On" and  
 207 "Off" state, respectively.

208 Fig. 4 shows the effect of changing the polymer thickness on the performance while  
 209 setting the field  $\frac{V_a}{t_p}$  to a certain constant (i.e.,  $\Delta n$  has a constant value). A constant  
 210 field is conserved by varying the  $V_a$  for different  $t_p$ . By doing this analysis, a  
 211 compromise between ER and  $E_{\text{bit}}$  is achieved.



212

213 **Fig. 4**  $E_{\text{bit}}$  versus polymer thickness ( $t_p$ ) for different MZI arm length

214 In addition, Fig. 4 shows the  $E_{\text{bit}}$  as a function of the  $t_p$  for constant  $\Delta n$  of  $6.35 \cdot 10^{-3}$   
 215 at different  $\zeta$ . The arrows show the positions of the maximum extinction ratio (ER)  
 216 for each  $\zeta$ . For a  $\zeta$  of 250  $\mu\text{m}$ , a maximum ER of 25.14 dB occurs for  $t_p$  of 50 nm  
 217 while for a  $\zeta$  of 350  $\mu\text{m}$ , a maximum ER of 23.02 occurs for  $t_p$  of 150 nm. The  
 218 previous study shows that for maintaining a maximum ER,  $t_p$  has to be increased with  
 219 increasing  $\zeta$ . On the other side, by changing  $t_p$  and  $\zeta$ ,  $V_\pi$  will change in which  $V_\pi$  is  
 220 0.25V at ( $\zeta = 250 \mu\text{m}$ ,  $t_p = 50 \text{ nm}$ ) while it is 0.52V at ( $\zeta = 350 \mu\text{m}$ ,  $t_p = 150 \text{ nm}$ )  
 221 which reflects the trade-off between  $E_{\text{bit}}$ , and ER, and  $V_\pi$  and the need to have an  
 222 optimized design to compromise between these performance metrics.

223 Table 1 shows the effect of applying different voltages and using different channel  
 224 lengths on the performance of the modulator in terms of the  $E_{\text{bit}}$ , ER, and  $V_\pi \zeta$  metrics  
 225 at  $\lambda_0 = 1550 \text{ nm}$ . As shown in the table, modulator performance varies based on the  
 226 design parameters selected for the optical design. From table 1, it could be  
 227 demonstrated that a polymer having a thickness of 150 nm at an applied voltage of 0.5  
 228 V represents the best compromise between ER and  $E_{\text{bit}}$ , and  $\zeta$  at a wavelength of 1550  
 229 nm with an ER = 20.36 dB,  $E_{\text{bit}} = 13.21 \text{ fJ/bit}$ , and  $\zeta = 350 \mu\text{m}$ .

230 Table 1. Different modulators design performance in terms of  $E_{\text{bit}}$ , ER, and  $V_{\pi}\zeta$  at  
 231  $\lambda_0 = 1550 \text{ nm}$ .

Applied Voltage (V)	Polymer Thickness $t_p$ (nm)	Energy per bit ( $E_{\text{bit}}$ ) (fJ/bit)	(ER) (dB)	Channel Length ( $\zeta$ ) ( $\mu\text{m}$ )	$V_{\pi}\zeta$ (V.cm)
2V	150	151.2	16.8	250	$1.83 \cdot 10^{-2}$
	150	211.7	20.1	350	$1.83 \cdot 10^{-2}$
1.5V	150	84.96	12.97	250	$1.83 \cdot 10^{-2}$
	150	118.94	23.02	350	$1.83 \cdot 10^{-2}$
1V	150	37.76	6.27	250	$1.83 \cdot 10^{-2}$
	150	52.86	22.44	350	$1.83 \cdot 10^{-2}$
0.5V	150	9.44	2.93	250	$1.83 \cdot 10^{-2}$
	150	13.21	20.36	350	$1.83 \cdot 10^{-2}$

232

233 A similar design was demonstrated in [7] in which an MZI based modulator with  
 234 ultra-thin silicon waveguide was fabricated. Although the design looks identical to the  
 235 proposed design here, the performance of both models is quite different. In [7], the  
 236 MZI-based modulator has a propagation loss of 4dB/cm compared to 0.024 dB/cm in  
 237 our paper. Owing to the high electro-optic coefficient of the polymer used here, we  
 238 believe the ER will surpass the achievable ER in [7] (i.e.,  $r_{33}=310 \text{ pm/v}$  in the  
 239 proposed work,  $r_{33}=70 \text{ pm/v}$  in [7]). Besides, we reach  $E_{\text{bit}}$  as low as 13.21 fJ/bit  
 240 compared to 30.18 fJ/bit. Table 2 shows the performance of the proposed MZI based  
 241 modulator as compared to silicon-based modulators previously proposed with  
 242 different structures. As shown, the proposed model is considered a good compromise  
 243 between each of ER and  $E_{\text{bit}}$ . Assuming low doping concentration, the resistivity of  
 244 silicon is around 10 Ohm.m. Whereas the waveguide has a thickness of 50 nm, and  
 245 the area equals  $350 \mu\text{m} \times 2 \mu\text{m}$ . The resistance is calculated to be 714 ohms. Hence,  
 246 the speed of the modulator can be estimated to be 17.66 GHz. The maximum  
 247 modulation bandwidth (f) that can be achieved is inversely proportional to the change  
 248 in the refractive index and is given by equation (5) [20]:

249 
$$(f * \zeta)_{\text{max}} = \frac{c}{4\Delta n} \quad (5)$$

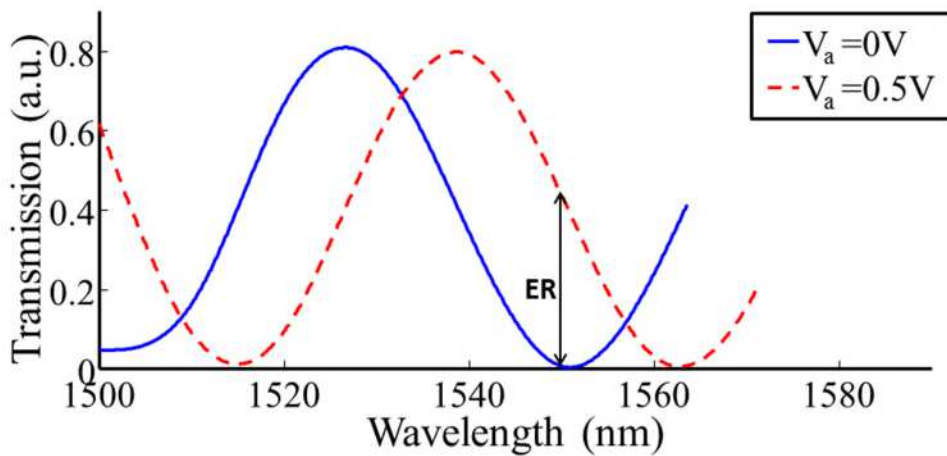
250 where  $c$  is the speed of light in air. From this equation, for  $\Delta n = 6.35 * 10^{-3}$ , and  
 251 arm length ( $\zeta$ ) of  $350 \mu\text{m}$ ,  $f_{max} = 3.37 * 10^{13}$  Hz.

252 Table 2. Comparison between the proposed structure and the previously proposed  
 253 silicon-based modulators.

Modulation principle	Modulator Structure	Extinction Ratio (ER) (dB)	Energy per bit ( $E_{bit}$ ) (fJ/bit)
Electro-Optic [7]	MZI	--	30.18 @ $V_a=2V$
Carrier Depletion [21]	MZI	3.8	147,000
Carrier Injection [22]	MZI	10	5,000
Carrier Injection [23]	Ring	7	120
Carrier Depletion [24]	Ring	6.5	50
Electro-refractive (proposed)	MZI	20.36	13.21

254

255 The transmitted intensity is plotted in Fig. 5 as a function of wavelength in which high  
 256 ER is achieved at 1550 nm with  $E_{bit} = 13.21$  fJ/bit [12, 13].



257

258 **Fig. 5** Transmission versus wavelength in the “On” and “Off” states.

## 259 4 CONCLUSION

260 MZI optical modulator based on the ultra-thin is presented in this paper. An MZI –  
261 based modulator is proposed. An extinction ratio of 20.36 dB at 1550 nm with an arm  
262 length of 350  $\mu\text{m}$  is reported. With an applied voltage of 0.5V, the low power  
263 consumption of 0.0158 W is achieved at high speed rates.

## 264 REFERENCES

- 265 1. Reed, G. T., et al. (2010). "Silicon optical modulators." *Nature Photonics* 4(8):  
266 518-526.
- 267 2. Ozbay, E. (2006). "Plasmonics: Merging Photonics and Electronics at Nanoscale  
268 Dimensions." *Science* 311(5758): 189.
- 269 3. Fernández Gavela, A., et al. (2016). "Last Advances in Silicon-Based Optical  
270 Biosensors." *Sensors* 16(3).
- 271 4. Cocorullo, G. and I. Rendina (1992) "Thermo-optical modulation at 1.5 $\mu\text{m}$  in  
272 silicon etalon." *Electronics Letters* 28, 83-85
- 273 5. Alloatti, L., et al. (2014). "100 GHz silicon–organic hybrid modulator." *Light:  
274 Science & Applications* 3(5): e173-e173.
- 275 6. Xiao, X., et al. (2013). "High-speed, low-loss silicon Mach–Zehnder modulators  
276 with doping optimization." *Optics Express* 21(4): 4116-4125.
- 277 7. Qiu, F., et al. (2015). "Ultra-thin silicon/electro-optic polymer hybrid waveguide  
278 modulators." *Applied Physics Letters* 107(12): 123302.
- 279 8. He, L., et al. (2012). "Ultrathin Silicon-on-Insulator Grating Couplers." *IEEE  
280 Photonics Technology Letters* 24(24): 2247-2249.
- 281 9. Zou, Z., et al. (2015). "60-nm-thick basic photonic components and Bragg  
282 gratings on the silicon-on-insulator platform." *Optics Express* 23(16): 20784-  
283 20795.
- 284 10. Abdeen, A. S., et al. (2016). High efficiency compact Bragg sensor. 2016  
285 *Photonics North (PN)*.
- 286 11. Ayoub, A. and M. Swillam (2017). Ultra-sensitive silicon-photonic on-chip sensor  
287 using microfabrication technology, SPIE.
- 288 12. Ayoub, A. and M. Swillam (2018). High-performance optical modulator using  
289 ultra-thin silicon waveguide in SOI technology, SPIE.

- 290 13. Ayoub, A. B. and M. A. Swillam (2017). High performance silicon Mach-Zehnder  
291 interferometer based photonic modulator. 2017 International Applied  
292 Computational Electromagnetics Society Symposium - Italy (ACES).
- 293 14. FDE tool: <https://www.lumerical.com/>
- 294 15. Baehr-Jones, T., et al. (2004). "High-Q ring resonators in thin silicon-on-  
295 insulator." Applied Physics Letters 85(16): 3346-3347.
- 296 16. Opti-FDTD, Opti-wave, Inc. <<http://www.optiwave.com>>.
- 297 17. Dalton, L. R., et al. (1995). "Polymeric Electro-Optic Modulators: Matereials  
298 synthesis and processing." Advanced Materials 7(6): 519-540.
- 299 18. Kim, T.-D., et al. (2007). "Ultralarge and Thermally Stable Electro-Optic  
300 Activities from Supramolecular Self-Assembled Molecular Glasses." Journal of  
301 the American Chemical Society 129(3): 488-489.
- 302 19. Timurdogan, E., et al. (2014). "An ultralow power athermal silicon modulator."  
303 Nature Communications 5(1): 4008.
- 304 20. Liu, J., et al. (2015). "Recent advances in polymer electro-optic modulators." RSC  
305 Adv. 5.
- 306 21. Liao, L., et al. (2005). "High speed silicon Mach-Zehnder modulator." Optics  
307 Express 13(8): 3129-3135.
- 308 22. Green, W. M. J., et al. (2007). "Ultra-compact, low RF power, 10 Gb/s silicon  
309 Mach-Zehnder modulator." Optics Express 15(25): 17106-17113.
- 310 23. Chen, L., et al. (2009). "Integrated GHz silicon photonic interconnect with  
311 micrometer-scale modulators and detectors." Optics Express 17(17): 15248-  
312 15256.
- 313 24. Dong, P., et al. (2009). "Low V<sub>pp</sub>, ultralow-energy, compact, high-speed silicon  
314 electro-optic modulator." Optics Express 17(25): 22484-22490.

315

316

### 317 **Biographies**

318 **Ahmed B. Ayoub** received his MS in physics from the American University in Cairo  
319 (AUC), Cairo, Egypt, in 2017. He is pursuing his Ph.D. in electrical engineering at the  
320 École Polytechnique Fédérale de Lausanne (EPFL), Lausanne, Switzerland. His  
321 current research interests include optical imaging, three-dimensional refractive index

322 reconstructions for biological samples, Plasmonic structures, Photonic integrated  
323 circuits, computational physics, and metamaterials. He is a member of OSA.

324

325

326 **Mohamed A. Swillam** received his Ph.D. from McMaster University, Hamilton,  
327 Canada, in 2008. After graduation, he worked as a postdoctoral fellow in the same  
328 group. In October 2009, he joined the photonic group and the Institute of Optical  
329 Sciences at the University of Toronto as a research fellow. In September 2011, he was  
330 appointed as an assistant professor at the Department of Physics, the American  
331 University in Cairo (AUC). His research interests include active and passive  
332 nanophotonic and plasmonic devices and systems, silicon photonics, metamaterials,  
333 and solar cells.

334

335

336

337

338

339 **Caption List:**

340

341 **Fig. 1** SOI ultra-thin waveguide structure. (a) Schematic for the physical dimensions  
342 of the ultra-thin waveguide. (b) Mode profile for the ultra-thin waveguide.

343 **Fig. 2** The effect of changing the waveguide width on the effective index. The  
344 substrate is assumed to be SiO<sub>2</sub> with air as the surrounding.

345 **Fig. 3** MZI photonic modulator. (a) Schematic for the ultra-thin waveguide based  
346 MZI modulator. (b) mode profile inside the polymer, it shows the strong interaction  
347 between the optical mode and the polymer.

348

349 **Fig. 4** E<sub>bit</sub> versus polymer thickness (**t<sub>p</sub>**) for different MZI arm length

350

351 **Fig. 5** Transmission versus wavelength in the “On” and “Off” states.

352

353 Table 1. Different modulators design performance in terms of  $E_{\text{bit}}$ , ER, and  $V_{\pi}\zeta$  at  
354  $\lambda_0 = 1550 \text{ nm}$  .

355 Table 2. Comparison between the proposed structure and the previously proposed  
356 silicon-based modulators.

357